Published online 24 January 2017

Nucleic Acids Research, 2017, Vol. 45, No. 9 ***5423–5436***
doi: 10.1093/nar/gkx051

Human BCDIN3D monomethylates cytoplasmic histidine transfer RNA

Anna Martinez[1], Seisuke Yamashita[1], Takashi Nagaike[1], Yuriko Sakaguchi[2], Tsutomu Suzuki[2] and Kozo Tomita[1,*]

[1]Department of Computational Biology and Medical Sciences, Graduate School of Frontier Sciences, The University of Tokyo, Kashiwa, Chiba 277-8562, Japan and [2]Department of Chemistry and Biotechnology, Graduate School of Engineering, The University of Tokyo, Bunkyo-ku, Tokyo 113-8656, Japan

Received November 12, 2016; Revised January 09, 2017; Editorial Decision January 18, 2017; Accepted January 19, 2017

ABSTRACT

Human RNA methyltransferase BCDIN3D is overexpressed in breast cancer cells, and is related to the tumorigenic phenotype and poor prognosis of breast cancer. Here, we show that cytoplasmic tRNA^{His} is the primary target of BCDIN3D in human cells. Recombinant human BCDIN3D, expressed in *Escherichia coli*, monomethylates the 5′-monophosphate of cytoplasmic tRNA^{His} efficiently *in vitro*. In BCDN3D-knockout cells, established by CRISPR/Cas9 editing, the methyl moiety at the 5′-monophosphate of cytoplasmic tRNA^{His} is lost, and the exogenous expression of BCDIN3D in the knockout cells restores the modification in cytoplasmic tRNA^{His}. BCIDN3D recognizes the 5′-guanosine nucleoside at position −1 (G_{-1}) and the eight-nucleotide acceptor helix with the G_{-1}–A_{73} mis-pair at the top of the acceptor stem of cytoplasmic tRNA^{His}, which are exceptional structural features among cytoplasmic tRNA species. While the monomethylation of the 5′-monophosphate of cytoplasmic tRNA^{His} affects neither the overall aminoacylation process *in vitro* nor the steady-state level of cytoplasmic tRNA^{His} *in vivo*, it protects the cytoplasmic tRNA^{His} transcript from degradation *in vitro.* Thus, BCDIN3D acts as a cytoplasmic tRNA^{His}-specific 5′-methylphosphate capping enzyme. The present results also suggest the possible involvement of the monomethylation of the 5′-monophosphate of cytoplasmic tRNA^{His} and/or cytoplasmic tRNA^{His} itself in the tumorigenesis of breast cancer cells.

INTRODUCTION

Bicoid-interacting protein 3 (BCDIN3) was initially isolated as a protein that interacts with the homeodomain-containing transcription factor, Bicoid, in *Drosophila* (1,2). BCDIN3 contains an S-(5′-adenosyl)-L-methionine (AdoMet) binding motif, and is homologous to a conserved family of eukaryotic protein methyltransferases acting on RNA-binding proteins (2,3). BCDIN3 is required for embryonic development in *Drosophila* (4). Subsequent studies revealed that the human BCDIN3 homolog monomethylates the 5′-γ-phosphate of 7SK RNA, a non-coding RNA involved in regulating the activity of the positive-acting transcription elongation factor, P-TEFb, a cyclin-dependent kinase complex (5,6). Monomethylation of the 5′-γ-phosphate of 7SK RNA protects 7SK from degradation and controls the activity of P-TEFb; therefore, BCDIN3 was renamed methylphosphate capping enzyme, MePCE (7,8).

The BCDIN3 Domain containing protein, BCDIN3D, is conserved from worm to human (9). The biological properties and function of BCDIN3D have not been characterized. BCDIN3D mRNA is overexpressed in human breast cancer cells, and the elevated expression of BCDIN3D is related to poor prognosis in breast cancer (10,11). Recently, it was reported that BCDIN3D dimethylates the 5′-monophosphate of specific precursor miRNAs (pre-miRNAs), such as the tumor suppressor miR145 (12–14), in MCF-7 breast cancer cells (9). Dimethylation of the 5′-monophosphate of the pre-miRNA negatively regulates the subsequent processing by Dicer *in vitro* (9,15), and results in the downregulated expression of the mature miRNA form. The shRNA-mediated depletion of BCDIN3D also reportedly results in the suppression of the tumorigenic phenotype of MDA-MB-231 breast cancer cells. Thus, BCDIN3D was proposed to promote the cellular invasion of breast cancer cells, by downregulating the expression of tumor suppressor miRNAs through the dimethylation of the 5′-monophosphate of the corresponding pre-miRNAs (9).

The mechanisms by which BCDIN3D recognizes specific pre-miRNAs and negatively regulates the expression of matured miRNAs in breast cancer cells are not well understood. To identify other possible target RNAs that are

*To whom correspondence should be addressed. Tel: +81 471 36 3611; Fax: +81 471 36 3611; Email: kozo_tomita@cbms.k.u-tokyo.ac.jp

methylated by BCDIN3D, and to clarify the mechanism by which BCDIN3D recognizes specific RNAs, we analyzed the BCDIN3D-binding RNAs in human HEK293T cells.

Here, we report that cytoplasmic histidyl tRNA ($tRNA^{His}$) is the primary target of BCDIN3D in HEK293T cells. We show that cytoplasmic $tRHA^{His}$ tightly binds to BCDIN3D *in vivo*, and the 5′-monophosphate of cytoplasmic $tRNA^{His}$ is monomethylated by BCDIN3D *in vitro* and *in vivo*. BCDIN3D monomethylates $tRNA^{His}$ more efficiently than pre-miR145 by over two orders of magnitude *in vitro*, and never dimethylates the 5′-monophosphates of $tRNA^{His}$ and pre-miR145. BCDIN3D recognizes the unique structures within cytoplasmic $tRNA^{His}$—the additional guanosine residue at position −1 (G_{-1}) and the eight-nucleotide acceptor helix with the G_{-1}–A_{73} mispair, which are exceptional features among cytoplasmic tRNA species. The monomethylation of the 5′-phosphate of cytoplasmic $tRNA^{His}$ protects it from degradation *in vitro*. Therefore, BCDIN3D acts as a cytoplasmic $tRNA^{His}$-specific 5′-methylphosphate capping enzyme. The involvement of the 5′-monophosphate methylation of cytoplasmic $tRNA^{His}$ and/or $tRNA^{His}$ itself in the tumorigenic phenotype of breast cancer cells is discussed.

MATERIALS AND METHODS

BCDINS3D-expressing stable cell lines

HEK293T and Flp-In™ T-REx™-293 cells were cultured in Dulbecco's modified Eagle's medium (DMEM) containing 10% FBS, under a humidified 5% CO_2 atmosphere at 37°C. The stable human cell line expressing streptavidin binding protein (SBP)-fused BCDIN3D (SBP-BCDIN3D) was established by Flp Recombinase-Mediated Integration (Flp-In system, Invitrogen, Japan), according to the manufacturer's instructions. The synthetic cDNA encoding human BCDIN3D was purchased from Eurofin Genomics, Japan, and was cloned into the pcDNA5/FRT/TO-Flag-HA-SBP vector (kind gift from Dr. Yamashita at Yokohama City University, Medical School). The resultant BCDIN3D expression plasmid, pcDNA5-SBP-BCDIN3D, was transfected into the host Flp-In™ T-REx™-293 cells, using Lipofectamine 2000 (Invitrogen, Japan). The cell line harboring pcDNA5-SBP-BCDIN3D was selected with hygromycin (100 μg/ml) and blasticidin (10 μg/ml) for two weeks, according to the manufacturer's instructions.

Preparation of SBP-BCDIN3D-associating RNAs

The stable cell lines expressing SBP-BCDIN3D were expanded to ten 10 cm plates, and SBP-BCDIN3D expression was induced by a treatment with 500 ng/ml of doxycycline for 48 h. The cell extracts were prepared with cell lysis buffer, containing 10 mM Tris–Cl, pH 8.0, 150 mM KCl, 10% (v/v) glycerol, 1% (v/v) Triton X-100, 5 mM DTT, 0.5 mM PMSF and complete protease cocktail (Roche, Japan) (buffer-A). SBP-BCDIN3D was purified using streptavidin beads (GE Healthcare, Japan). The beads were washed with buffer-A, and SBP-BCDIN3D was eluted by buffer-A containing 2 mM biotin (Sigma-Aldrich, Japan). The SBP-BCDIN3D associating RNAs were prepared using ISOGEN II (Nippon Gene, Japan), and separated by 10% (w/v) polyacrylamide gel electrophoresis under denaturing conditions, and the gel was stained with SYBR-Gold Nucleic Acid Stain (Invitrogen, Japan).

Mass spectrometric analysis of RNAs

The gel-purified RNA was digested by RNases, and the resultant RNA fragments were analyzed by capillary LC-nano ESI-mass spectrometry, as described previously (16,17). The gel-purified RNA-x (0.1 μg) was digested with RNase T_1 (Epicentre) or RNase A (Ambion) and analyzed by an LTQ Orbitrap mass spectrometer (ThermoFisher Scientific, Japan), with a nano-electrosprayer connected to a splitless nanoflow high pressure liquid chromatography system (DiNa, KYA Technologies).

Expression and purification of BCDIN3D in *E. coli*

The DNA encoding human BCDIN3D was cloned between the Nde I and Xho I sites of the pET15b vector (Novergen, Japan). *Escherichia coli* BL21(DE3) cells were transformed by the plasmid and grown in LB medium containing 50 μg/ml ampicillin at 37°C until the A_{600} reached 0.8, and the expression of histidine-tagged BCDIN3D was induced by the addition of IPTG (isopropyl-β-D thiogalactopyranoside) at a final concentration of 0.1 mM for 12 h at 20°C. The cells were harvested, sonicated in buffer containing 50 mM Tris–Cl, pH 7.0, 500 mM NaCl, 5 mM β-mercaptoethanol, 10 mM imidazole and 10% (v/v) glycerol (buffer-B), and centrifuged at 100 000 *g* for 1 h at 4°C. The clear supernatant was applied to a Ni^{2+}-NTA agarose column (QIAGEN, Japan) equilibrated with buffer-B. The column was washed with buffer-B, and the protein was eluted with buffer containing 50 mM Tris–Cl, pH 7.0, 500 mM NaCl, 5 mM β-mercaptoethanol and 400 mM imidazole. The protein was further purified by chromatography on Hi-Trap Q and Hi-Trap Heparin columns (GE Healthcare, Japan). Finally, the protein was purified by chromatography on a Hi-Load 16/60 Superdex 200 column (GE Healthcare, Japan), in buffer containing 25 mM Tris–Cl, pH 7.0, 200 mM NaCl and 10 mM β-mercaptoethanol, concentrated to 3 mg/ml and stored at −80°C. The catalytically inactive BCDIN3D protein with the D72A/G74A mutations was also prepared as described above.

In vitro methylation assay

In vitro methylation of RNAs was carried out by the trichloroacetic acid (TCA) precipitation of reaction products. For standard assays using ^{14}C-S-adenosylmethionine (AdoMet), a reaction mixture (80 μl volume) containing 50 mM Tris–Cl, pH 7.9, 50 mM KCl, 5 mM $MgCl_2$, 0.1 mM EDTA, 2 mM DTT, 5 % (v/v) glycerol, 2 μM RNA, 50 μM [^{14}C]-AdoMet (40 mCi/mmol, PerkinElmer, Japan), and 0.1 μM BCDIN3D was incubated at 37°C. An aliquot (10 μl) was withdrawn at the indicated time from the reaction solution and spotted onto a Whatman 3MM filter (GE Healthcare, Japan) that was pre-soaked with cold 10% (w/v) TCA. After the filters were washed with cold 10% (w/v) TCA, they were washed with ethanol and dried.

The filters were suspended in Ultima Gold liquid scintillation cocktail (PerkinElmer, Japan) in vials, and the radioactivities on the filters were quantified with a liquid scintillation counter (Beckman Coulter). To visualize the ^{14}C-methylated RNA products, after the reaction, the RNAs were purified by phenol–chloroform treatment, followed by ethanol precipitation, and separated by 10% (v/v) polyacrylamide gel electrophoresis under denaturing conditions. The gel was dried and exposed to an imaging plate for 16 h, and the intensities of the methylated RNAs were quantified with a BASS2000 imager (Fujifilm, Japan). For kinetic analysis, the specific activity of ^{3}H-AdoMet (55 Ci/mmol, PerkinElmer, Japan) was adjusted to 1.1 Ci/mol (500 μM) with non-radiolabeled AdoMet (Sigma-Aldrich, Japan), and used for the assays. Reaction mixtures (10 μl), containing 50 mM Tris–Cl, pH 7.9, 50 mM KCl, 5 mM $MgCl_2$, 0.1 mM EDTA, 2 mM DTT, 5 % (v/v) glycerol, 50 μM [^{3}H]-AdoMet (1.1 Ci /mmol), 0.1 μM BCDIN3D, and various concentrations of RNAs (0.125–15 μM), were incubated at 37°C for 10 min. RNA substrates (pre-miR145, $tRNA^{His}$, $tRNA^{Phe}$ and their variants) were synthesized, using plasmids encoding the respective template DNA sequences downstream of the T7 promoter, by T7 RNA polymerase in the presence of excess GMP, and were purified by 10% (w/v) polyacrylamide gel electrophoresis under denaturing conditions. The RNA mini-helices corresponding to the top-half of cytoplasmic $tRNA^{His}$, with 5′-monophosphate and its variants (Supplementary Table S1), were purchased from FASMAC, Japan.

Construction of BCDIN3D knockout cells by CRISPR/Cas9

BCDIN3D knockout cells were generated by the CRISPR-Cas9 system (18). Oligonucleotides encoding sgRNAs (sgRNA1 or sgRNA2), which target exon 1 of the BCDIN3D gene, were cloned into the pX330 (Addgene plasmid 42230) vector (19). The nucleotide sequences of the oligonucleotides encoding the sgRNAs are shown in Supplementary Table S1. HEK293T cells were seeded into 24-well plates at a density of 250 000 cells per well, and were used for transfection. Cells were transfected with 300 ng of PX330 containing the sgRNA sequence, 100 ng of pLL3.7-puro and 100 ng of pEGFP-N1, using Lipofectamine 3000 (Life Technologies, Japan) according to the manufacturer's protocol. After 24 h, the transfection efficiency was estimated from the fraction of fluorescent cells, and transfected cells were selected by adding 5 μg/ml of puromycin (Sigma Aldrich) for 5 days. After 5 days, the cells were diluted to obtain isolated clones. The isolated HEK293T cells were further transfected with PX330 containing the sgRNA sequence, to enhance the possibility of obtaining BCDIN3D knockout cells, and isolated clones were obtained as described above. The knockouts of the BCDIN3D gene were confirmed by DNA sequencing of PCR fragments spanning the target sites, and the lack of BCDIN3D expression in the isolated cells was confirmed by western blotting using an anti-BCDIN3D antibody (Sigma Aldrich). Cytoplasmic $tRNA^{His}$ species were isolated from total tRNA fractions, prepared from HEK293T and BCDIN3D knockout cells, by the solid-phase hybridization method (20–22). The 3′-biotinylated oligonucleotide probe, with the sequence complementary to the 3′-terminal 30 nucleotides of cytoplasmic $tRNA^{His}$ (5′-CCGTGACTCGGATTCGAACCGAGGTTGCTG-biotin-3′), was purchased from Eurofins, Japan. The isolated $tRNA^{His}$ species were further purified by 10% (v/v) polyacrylamide gel electrophoresis under denaturing conditions.

Measurement of cell growth

For measurement of cell growth, HEK293T, KO1 and KO2 cells were seeded in a 96-well plate (2500 cells/ well; 100 μl medium) and cultured at 37°C. Cell proliferation was measured using a CellTiter-Blue Cell Viability Assay (Promega, Japan), according to the manufacturer's instructions. At the indicated times (1, 2, 3 and 4 days), the CellTiter-Blue Reagent (20 μl/well) was added, and the cells were incubated for 1 h before recording the fluorescence (560Ex/590Em), using a GloMax Multi-Detection System (Promega, Japan).

In vitro aminoacylation assay

The $tRNA^{His}$ transcript with the 5′-monophospate was methylated by BCDIN3D *in vitro*, and the resultant $tRNA^{His}$ with a 5′-monomethylphosphate was gel-purified. The fraction of methylated $tRNA^{His}$ ($tRNA^{His}\_pmG_{-1}$) was found to be more than 99%, as revealed by the LC–mass spectrometric analysis. The DNA encoding human histidine tRNA synthetase (HisRS) lacking the C-terminal three amino acids (C507I508C509) was cloned between the Nde I and Xho I sites of the pET15b vector (Novagen, Japan). The hexa-histidine-tagged HRS was expressed in *Escherichia coli* BL21(DE3) cells, and purified as described above. Reaction solutions containing 50 mM Tris–Cl, pH 7.6, 100 mM KCl, 10 mM $MgCl_2$, 8 mM DTT, 2.5 mM ATP, 60 μM L-[^{14}C]-histidine (320 mCi/mmol, PerkinElmer, Japan), $tRNA^{His}$ variants (0–7.5 μM) and 5 nM HisRS were incubated at 37°C for 10 min. The reaction solutions were spotted onto Whatman 3MM filters (GE Healthcare, Japan) pre-soaked with cold 10% (w/v) TCA. The filters were washed with cold 10% (w/v) TCA, and then with ethanol and dried. The radioactivities on the filters were quantified as described above.

Northern blotting

Total RNAs or smaller RNAs (shorter than 200 nucleotides) from human cells were purified with the Isogen-II (Nippon Gene, Japan) or NucleoSpin miRNA (Takara, Japan) reagent, according to the manufacturer's protocol. The RNAs (2.5–10 μg) were separated by 10% (v/v) polyacrylamide gel electrophoresis under denaturing conditions, and blotted onto a Hybond-N+ membrane (GE Healthcare, Japan) using a Trans-Blot SD semi-dry Electrophoretic Transfer Cell (Bio-Rad, Japan), according to the manufacturer's protocol. Hybridization was performed overnight at 55°C in PerfectHyb Hybridization solution (Toyobo, Japan), using 5′-^{32}P-labeled oligo DNA probes. The membrane was washed three times in 2 × standard

saline citrate (SSC) and 0.1% (w/v) SDS at 55°C for 20 min. The DNA sequences used as specific probes are shown in Supplementary Table S1.

Quantitative PCR

Smaller RNAs (shorter than 200 nucleotides) from human cells were purified, as described above. The expression level of mature miR145 relative to that of U6 snRNA was quantified by using a TaqMan MicroRNA Assay (Applied Biosystems, Japan). The RNA (10 ng) was used for reverse transcription (RT, 15 μl reaction solution) with a Taqman MicroRNA Reverse Transcription kit (Applied Biosystems, Japan). After RT, qPCR was performed using 0.75 μl of the RT solution with Taqman Universal Master mix II (Applied Biosystems, Japan, 10 μl reaction solution). The expression level of pre-miR145 relative to that of U6 snRNA was quantified by qPCR, using pre-miR145-specific primers (Supplementary Table S1). For RT (10 μl reaction solution), 10 ng RNA was incubated with Primescript RT kit (Perfect Real Time (Takara, Japan) reagents. After RT, qPCR was performed using 1 μl of RT solution and SYBR Premix Ex Taq II (Takara, Japan, 20 μl reaction solution).

In vitro decay of tRNAs

The $tRNA^{His}$ transcript (1 μg) was dephosphorylated by bacterial alkaline phosphatase (BAP; Takara, Japan), and was 5′-^{32}P-labeled by T4 polynucleotide kinase (PNK; Toyobo, Japan) and γ-[^{32}P]-ATP (3000 Ci/mmol, PerkinElmer, Japan). The 5′-^{32}P labeled $tRNA^{His}$ (5′p-$tRNA^{His}$) was methylated by recombinant BCDIN3D, resulting in the synthesis of 5′mp-RNA^{His}. The 5′p-$tRNA^{His}$ and 5′mp-$tRNA^{His}$ were further purified by acrylamide gel electrophoresis under denaturing conditions. The cytoplasmic fraction of HEK293T cells was prepared with NE-PER™ Nuclear and Cytoplasmic Extraction Reagents (Thermo Fisher Scientific, Japan), according to the manufacturer's protocol, and the concentration of proteins in the extracts was quantified by a Bradford assay (Bio-Rad, Japan), using BSA as the standard. The reaction mixtures (90 μl), containing 20 mM Tris–Cl, pH 8.0, 100 mM KCl, 3.2 mM $MgCl_2$, 1mM DTT, 140 μg cytoplasmic protein and 10 000 cpm 5′-p$tRNA^{His}$ (or 5′-mptRNA^{His}), were incubated at 37°C. At the indicated times (0, 10, 20, 30, 60, 90, 120 and 150 min), an aliquot (10 μl) was withdrawn from the solution, and the RNA was purified by phenol-extraction and ethanol-precipitated. The RNAs were separated by 10% (w/v) polyacrylamide gel electrophoresis under denaturing conditions. The intensities of the intact RNA were quantified with a BASS2000 imager (Fujifilm, Japan).

RESULTS

Cytoplasmic $tRNA^{His}$ associates with BCDIN3D *in vivo*

To identify RNA species that interact with BCDIN3D, a HEK293T cell line stably expressing streptavidin binding protein (SBP)-tagged BCDIN3D (SBP-BCDIN3D) was established. The SBP-BCDIN3D in the cell extracts was bound to streptavidin beads, and SBP-BCDIN3D was eluted from the beads by biotin (Figure 1A). The electrophoretic analysis of the RNA species that co-purified with SBP-BCDIN3D revealed a distinct RNA with a 70–80 nucleotide length (named RNA-x) that co-purified with SBP-BCDIN3D, but not with the control SBP (Figure 1B). This suggested that RNA-x specifically binds to BCDIN3D or BCDIN3D-associating proteins.

Over thirty years ago, human and fruit fly cytoplasmic histidyl tRNAs ($tRNA^{His}$s) were reported to have a 5′-monomethylmonophosphate (23,24), and BCDIN3D is localized in the cytoplasm in human cells (9). Thus, we presumed that RNA-x is a cytoplasmic $tRNA^{His}$. RT-PCR of the RNA fractions that co-purified with BCDIN3D, using primers specific to cytoplasmic $tRNA^{His}$, indicated that the cytoplasmic $tRNA^{His}$ co-purified with BCDIN3D, but not with the control SBP from the cell extracts (Figure 1C). DNA sequencing of the RT-PCR product, amplified using $tRNA^{His}$-specific primers, confirmed that cytoplasmic $tRNA^{His}$ indeed co-purified with BCDIN3D. In contrast, cytoplasmic $tRNA^{Phe}$ did not co-purify with BCDIN3D. RT-PCRs also confirmed that neither $tRNA^{His}$ nor $tRNA^{Phe}$ was co-purified with SBP. Thus, RNA-x was identified as cytoplasmic $tRNA^{His}$.

To substantiate the results, RNA-x was digested with RNase T_1 and subjected to capillary LC-nano ESI-MS analysis (16,25). The series of RNA fragments were definitively assigned to the entire sequence of cytoplasmic $tRNA^{His}$ with post-transcriptional modifications (23) (Figure 1D, Supplementary Figure S1A–C). To detect the 5′ terminal fragment of $tRNA^{His}$, RNA-x was digested with RNase A. An RNA fragment with a molecular mass corresponding to the 5′-terminal trimer with monomethylation, 5′-mpGGCp (mp: monomethylmonophosphate; m/z 1,106), of cytoplasmic $tRNA^{His}$ was identified (Figure 1D, E, Supplementary Figure S1D). No RNA fragment with a molecular mass corresponding to either the unmethylated fragment (5′-pGGCp, m/z 1092) or the dimethylated fragment (5′-m_2pGGCp; m/z 1120) was detected. Collision-induced dissociation (CID) spectrometric analysis of the fragment confirmed the presence of a methyl-group at the 5′-terminal monophosphate of cytoplasmic $tRNA^{His}$ (Figure 1F), as previously reported (23). Together, our results showed that cytoplasmic $tRNA^{His}$ binds to BCDIN3D or its associated proteins, and has a 5′-monomethylmonophosphate. These results prompted us to analyze cytoplasmic $tRNA^{His}$ as a substrate of BCDIN3D.

BCDIN3D monomethylates the 5′-phosphate of $tRNA^{His}$ *in vitro*

To examine whether BCDIN3D can methylate the 5′-monophosphate of cytoplasmic $tRNA^{His}$ *in vitro*, BCDIN3D was overexpressed in *E. coli*, purified and tested for its activity, using a cytoplasmic $tRNA^{His}$ transcript as the substrate and S-(5′-adenosyl)-L-methionine (AdoMet) as the methyl-group donor. The *in vitro* methylation assay demonstrated that wild-type BCDIN3D transfers the methyl group of AdoMet to $tRNA^{His}$ efficiently in a time-dependent manner (Figure 2A), under standard conditions. The catalytically-inactive mutant protein, BCDIN3D-D72A/G74A, does not transfer the methyl group of AdoMet $tRNA^{His}$ at all (Supplementary Fig-

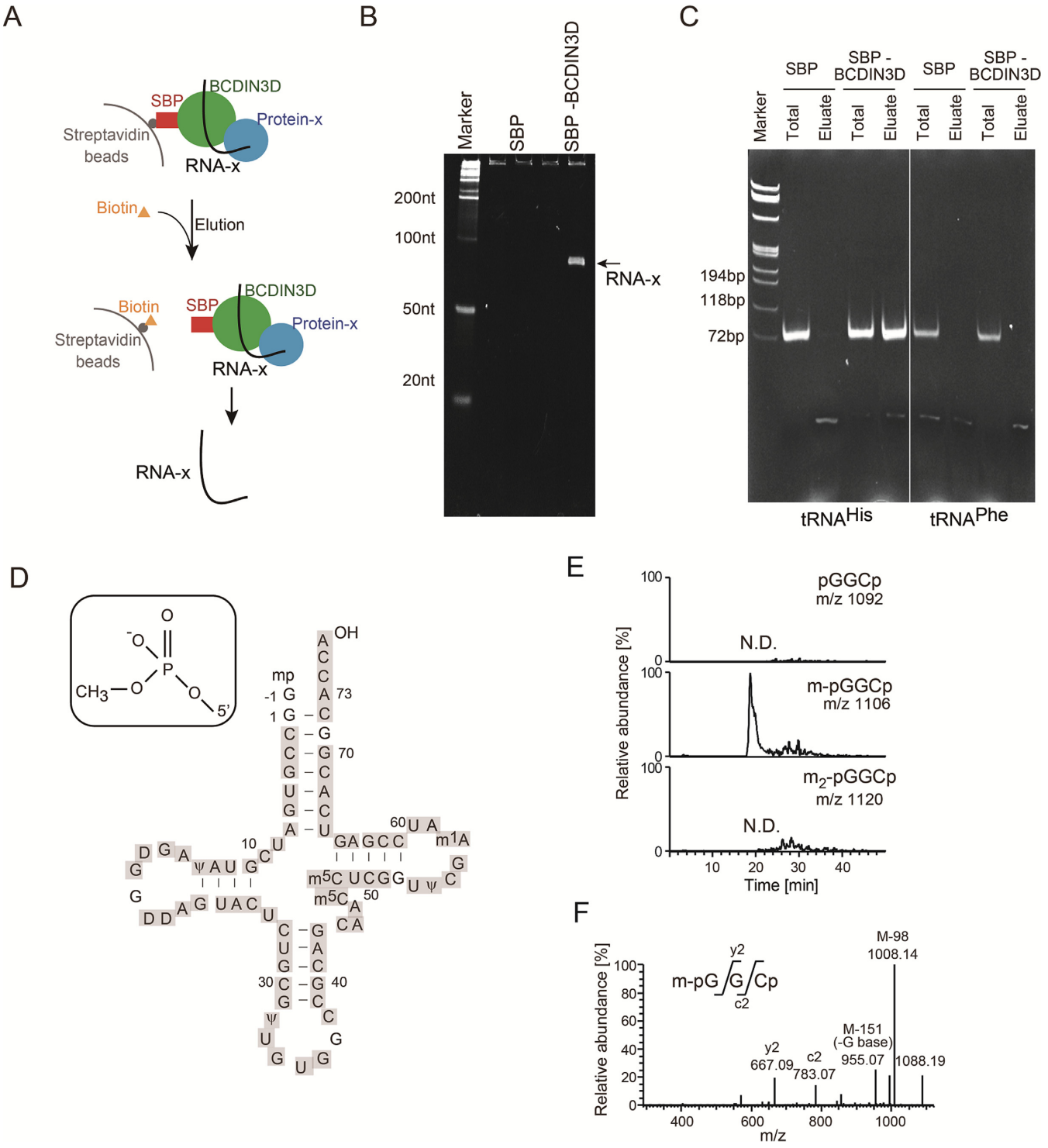

Figure 1. Cytoplasmic $tRNA^{His}$ binds to BCDIN3D or its associated protein(s) and has 5′-monomethylmonophosphate. (**A**) Schematic presentation of the isolation of RNAs interacting with BCDIN3D. (**B**) Electrophoretic analysis of the RNA fraction co-purified with SBP-BCDIN3D (SBP-BCDIN3D, right lane), and control SBP (SBP, left lane) from cell extracts. The arrow indicates RNA-x specifically bound to BCDIN3D or its associated protein(s). (**C**) RT-PCR of RNAs interacting with BCDIN3D. Total RNAs from SBP-BCDIN3D- or SBP-expressing cells or RNAs co-purified with SBP-BCDIN3D or SBP were subjected to RT-PCR, using $tRNA^{His}$- (left) or $tRNA^{Phe}$- (right) specific primers. (**D**) Nucleotide sequence of human cytoplasmic $tRNA^{His}$ (23). LC/MS analysis of RNase T1-digested fragments of RNA-x identified cytoplasmic $tRNA^{His}$ (Supplementary Figure S1A–C). The fragments cover the sequences of cytoplasmic $tRNA^{His}$ (grey-shaded). (**E**) LC/MS analysis of RNase A-digested fragments of RNA-x. Identification of the molecular mass corresponding to 5′pmG_{-1}-G_1-C_2 p (pmG: guanosine 5′-monomethyl monophosphate; m/z 1,106) of cytoplasmic $tRNA^{His}$ (Supplementary Figure S1D). (**F**) Collision-induced dissociation (CID) spectrum of the RNA fragment of 5′pmG_{-1}-G_1-C_2 p in (E), showing that a methyl-group is attached to the 5′-monophosphate of $tRNA^{His}$.

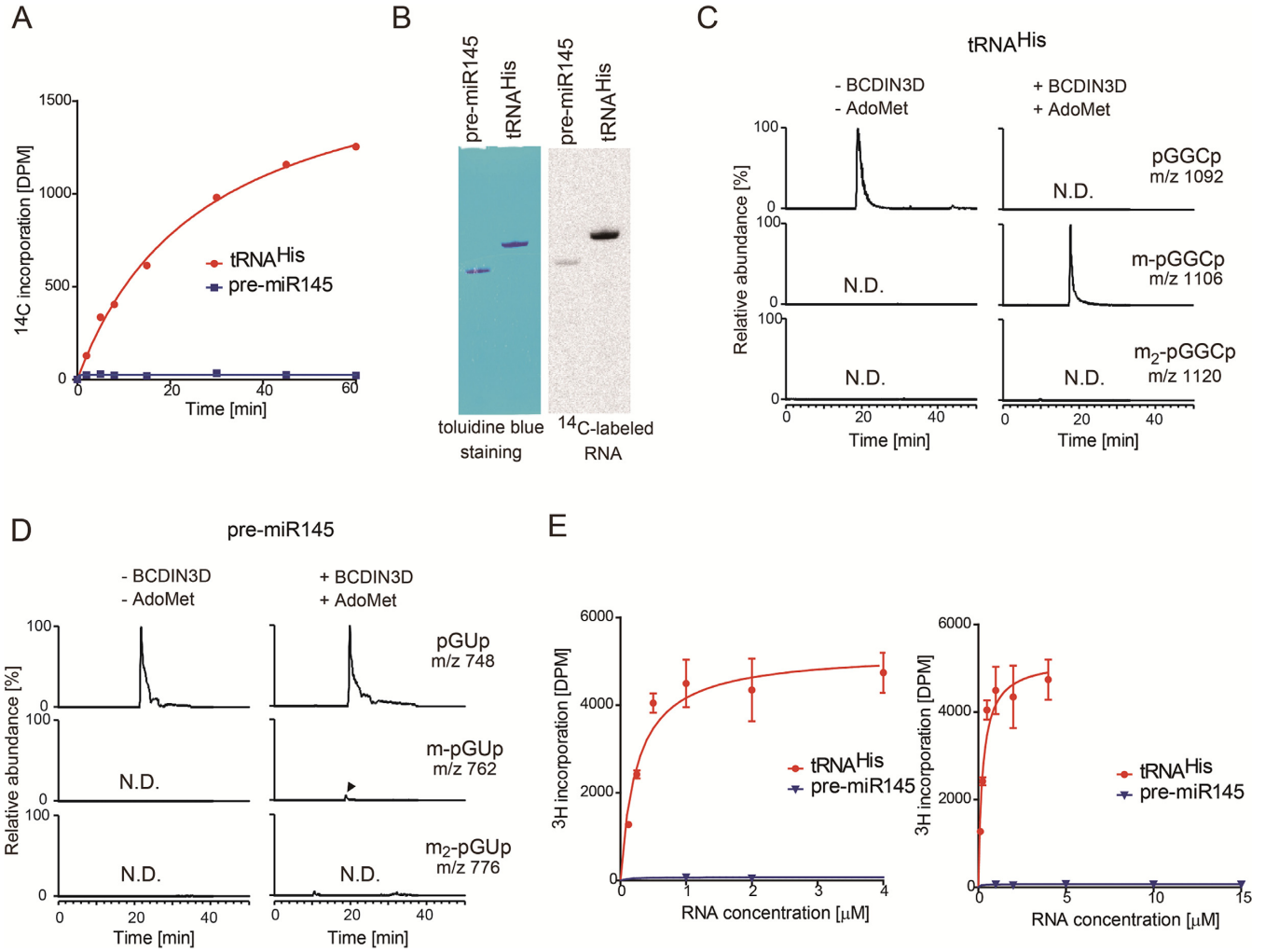

Figure 2. Monomethylation of 5′-monophosphate of tRNA^{His} by BCDIN3D *in vitro*. (**A**) *In vitro* methylation of tRNA^{His} and pre-miR145 transcripts. Time courses of methyl-group transfer from AdoMet to tRNA^{His} and pre-miR145 transcripts under standard conditions (2 μM RNA substrate and 0.1 μM recombinant BCDIN3D). (**B**) *In vitro* methylation of tRNA^{His} and pre-miR145 with a higher concentration of BCDIN3D (1 μM) at 37°C for 2 h. After the reaction, the RNA was separated by 10% (v/v) polyacrylamide gel electrophoresis under denaturing conditions. The gel was stained with toluidine blue (left), dried and exposed to a BASS2000 imaging plate (Fujifilm, Japan) for 12 hours (right). Mass spectrometric analysis of the RNase A-digested products of BCDIN3D-treated. (**C**) tRNA^{His} and (**D**) pre-miR145. (**E**) The steady state kinetics of methylation of tRNA^{His} and pre-miR145. Reaction mixtures containing various concentrations of tRNA^{His} (0.125–4 μM; left) and pre-miR145 (1–15 μM; right) were incubated at 37°C for 10 min. The bars in the graphs are SD of more than two independent experiments.

ure S2A and B). This excludes the possibility that the observed methylation of tRNA^{His} by BCDIN3D is due to contamination by other methyltransferases in *E. coli*. Recently, BCDIN3D was reported to dimethylate the 5′-monophosphates of a specific group of miRNA precursors (pre-miRNAs), such as pre-miR145. The dimethylation of the 5′-phosphate of pre-miR145 negatively regulates the following Dicer processing (9). However, the methyl group of AdoMet is not significantly transferred to pre-miR145, as compared with tRNA^{His}, under the tested conditions (Figure 2A).

Under conditions with larger amounts of recombinant BCDIN3D and a prolonged incubation time, a slight amount of the methyl group is transferred to pre-miR145, as detected with a phosphorimager, but the efficiency is much lower than that of tRNA^{His} (~1%, Figure 2B). LC-mass spectrometric analyses of RNaseA-treated reaction products confirmed that the 5′-monophosphate of tRNA^{His} is fully monomethylated, and the 5′-monophosphate of the pre-miRNA transcript is monomethylated with lower efficiency. Neither tRNA^{His} nor pre-miR145 was dimethylated *in vitro* (Figure 2C and D).

The steady-state kinetics analyses of the methylation of the 5′-monophosphates of tRNA^{His} and pre-miR145 provided estimated K_m values for tRNA^{His} and pre-miR145 of 0.25 μM and >>15 μM, respectively (Figure 2E), and the V_{max} value of pre-miR145 was much lower than that of tRNA^{His}. Therefore, cytoplasmic tRNA^{His} is a much better substrate of BCDIN3D than pre-miR145, by over two to three orders of magnitude, *in vitro*. Thus, the primary target of BCDIN3D is cytoplasmic tRNA^{His}, rather than pre-miRNAs, and BCDIN3D has monomethylation activity acting on the 5′-monophosphate of cytoplasmic tRNA^{His}.

BCDIN3D monomethylates the 5′-phosphate of tRNA^{His} *in vivo*

To determine whether the monomethylation of the 5′-monophosphate of cytoplasmic tRNA^{His} occurs under normal physiological conditions, cytoplasmic tRNA^{His} was purified from HEK293T cells, using an oligonucleotide probe complementary to cytoplasmic tRNA^{His}. The purified cytoplasmic tRNA^{His} was analyzed by LC-mass spectrometry (Supplementary Figure S3). Quantification of the methylation of the 5′-monophosphate of cytoplasmic tRNA^{His} confirmed that 99% of the cytoplasmic tRNA^{His} has the 5′-monomethylmonophosphate. This suggests that, under normal physiological conditions, the 5′-monophsphate of cytoplasmic tRNA^{His} is almost fully monomethylated.

Next, to examine the monomethylation of the 5′-monophosphate of tRNA^{His} by BCDIN3D *in vivo*, the BCDIN3D gene in the HEK293T genome was knocked out, using the clustered regulatory interspaced short palindromic repeat CRISPR/Cas9 system (19,26). Two knockout cell lines were obtained (KO1 and KO2). Both KO cell lines have nucleotide deletions in exon-1 of the BCDIN3D gene, which lead to the frame-shift mutation of the BCDIN3D mRNA (Figure 3A). The absence of BCDIN3D protein expression in the knockout cells was confirmed by western blotting (Figure 3B). The knockout of BCDIN3D slightly impairs the growth of HEK293T cells (Supplementary Figure S4A).

Small RNA fractions were prepared from wild-type HEK293T, KO1 and KO2 cells (Figure 3C, left), and subjected to *in vitro* methylation by recombinant BCDIN3D. While the RNA fractions from HEK293T cells were not significantly methylated, those from the KO1 and KO2 cells were methylated (Figure 3C, right). The length of the ^{14}C-labeled RNA corresponds to that of tRNAs, and no other RNA smaller or larger than the tRNA fractions was ^{14}C-labeled. The cytoplasmic tRNA^{His} was further purified from the total tRNA fractions of wild-type HEK293T and KO cells, and subjected to *in vitro* methylation using recombinant BCDIN3D (Figure 3D). The tRNA^{His} purified from HEK293T cells was barely methylated by BCDIN3D *in vitro*, confirming that most of the cytoplasmic tRNA^{His} fraction from the cells bears the 5′-monomethylmonophosphate *in vivo* (Supplementary Figure S3). In contrast, the cytoplasmic tRNA^{His} species purified from the KO cells are methylated *in vitro*. These results suggest that BCDIN3D is responsible for the methylation of tRNA^{His} *in vivo*. Analyses by qPCR also confirmed that the expression levels of the 7SK-specific methyltransferase, BCDIN3, in BCDIN3D-knockout cells are not affected (Supplementary Figure S4B). This excludes the possibility that BCDIN3 is involved in the methylation of tRNA^{His} *in vivo*.

The tRNA^{His} species from rescued KO cells, in which BCDIN3D was exogenously expressed, are also methylated, but the efficiencies are about half of those of tRNA^{His} from KO cells. This suggests that BCDIN3D methylates cytoplasmic tRNA^{His} *in vivo*. The exogenous expression levels of SBP-BCDIN3D in KO1 and KO2 were much higher than the endogenous expression of BCDIN3D in wild-type HEK293T cells (Supplementary Figure S5). Thus, the modest effect (∼ 50%) of the exogenous expression of BCDIN3D in KO cells on the methylation is probably due to the transfection efficiencies of the BCDIN3D plasmid in the KO cells. The cytoplasmic tRNA^{His} species isolated from these cells were further analyzed by LC-mass spectrometry (Figure 3E, F). The results confirmed that, in KO cells, the cytoplasmic tRNA^{His} lacks the 5′-monomethylmonophosphate, and only the 5′-monophosphate form of tRNA^{His} is observed. Furthermore, in the rescued KO cells, tRNA^{His} with the 5′-monomethylmonophosphate is restored. Thus, BCDIN3D is responsible for the monomethylation of the 5′-monophosphate of cytoplasmic tRNA^{His} *in vivo*.

Recognition of cytoplasmic tRNA^{His} by BCDIN3D

Human cytoplasmic tRNA^{His} has unique features, among cytoplasmic tRNA species. After the 5′-leader is removed from the precursor tRNA^{His} transcript by an endonuclease, an extra guanosine residue (G_{-1}) is attached to the 5′-end by tRNA^{His} guanyltransferase (Thg) (27). As a result, the mature cytoplasmic tRNA^{His} has an eight-nucleotide acceptor helix with a protruding $C_{74}C_{75}A_{76}$ sequence, but G_{-1} does not base-pair with the A_{73} discriminator nucleotide (Figure 1D). In contrast, all other canonical cytoplasmic tRNA species have a seven-nucleotide acceptor helix.

To evaluate the substrate requirement for the methylation of cytoplasmic tRNA^{His} by BCDIN3D, mutation(s) or deletion was introduced into the tRNA^{His} transcript (Figure 4A-D), and the steady-state kinetics were analyzed. The tRNA^{His} mutant lacking G_{-1} (tRNA^{His}_ΔG_{-1}) and that with the A_{73}C mutation (tRNA^{His}_A_{73}C) were quite poor substrates for BCDIN3D, suggesting that the G_{-1} and G_{-1}–A_{73} mis-pair are required for the methylation of the 5′-monophosphate of tRNA^{His} (Figure 4B). The methylation efficiencies of tRNA^{His} mutants lacking either $C_{74}C_{75}A_{76}$ (tRNA^{His}_ΔCCA) or the G_6:C_{67} base pair in the acceptor stem (tRNA^{His}_ΔG_6-C_{67}) were reduced to ∼30% of that of wild-type tRNA^{His}. The reduced methylation efficiencies arise from the lower affinities of the mutant tRNAs (Figure 4B, D): the K_m values of tRNA^{His}_ΔCCA and tRNA^{His}_ΔG_6:C_{67} are increased by factors of four and three as compared to that of wild-type tRNA^{His}, respectively (Figure 4D). In contrast, the methylation efficiency of the tRNA^{His} mutant lacking the anticodon loop (tRNA^{His}_Δ32–35) is actually slightly better than that of wild-type tRNA^{His}. Furthermore, while the wild-type tRNA^{Phe} transcript does not function as a substrate for BCDIN3D, the introduction of an extra G (G_{-1}) at the 5′ end of tRNA^{Phe} (tRNA^{Phe}_G_{-1}) increases the methylation efficiency to ∼40% of that of tRNA^{His} (Figure 4C, D). In addition, the V_{max} value is almost the same as that of tRNA^{His}.

Moreover, the tRNA^{His} mini-helix is also methylated efficiently. Thus, the top half of tRNA^{His}, especially the acceptor helix, is recognized by BCDIN3D (Figure 4E). The nucleotide preference at position -1 of the tRNA^{His} mini-helix by BCDIN3D was also analyzed, using tRNA^{His} mini-helix variants (Figure 4F, G). The tRNA^{His} mini-helices with A_{-1}, C_{-1} and U_{-1} were methylated less efficiently than the wild-type tRNA^{His} mini-helix with G_{-1}. The methylation efficiencies of tRNA^{His} mini-helices with A_{-1}, C_{-1} and U_{-1}

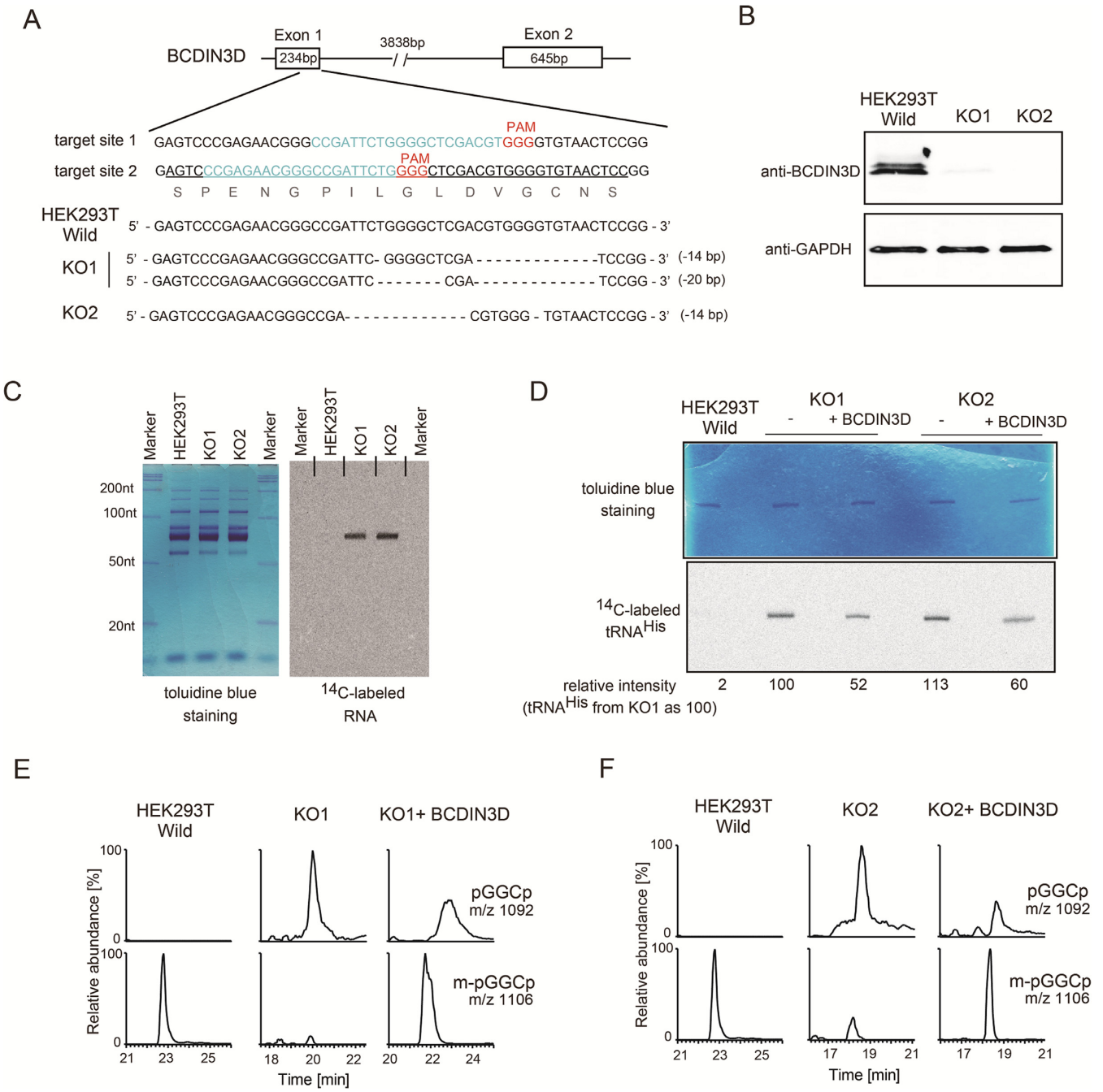

Figure 3. BCDIN3D monomethylates the 5′-monophosphate of $tRNA^{His}$ *in vivo*. (**A**) Schematic representation of the location of guide RNAs (gRNA1 and gRNA2) targeting the BCDIN3D gene locus. The nucleotide sequence of the region surrounding the target site (upper), and those of the regions surrounding the targeted deletion sites in knockout cells (KO1 and KO2, lower) for cleavage by CRISPR/Cas9. (**B**) Expression of the BCDIN3D protein in wild-type HEK293T cells and BCDIN3D knockout cells (KO1 and KO2). The BCDIN3D protein was detected by western blotting, using an anti-BCDIN3D antibody. GAPDH expression was used as a positive control. (**C**) Small RNA fractions were prepared from wild-type HEK293T cells and BCDIN3D KO cells (KO1 and KO2). The RNAs were subjected to *in vitro* methylation by BCDIN3D, as in Figure 2B, using 5 μg small RNA fractions, and the reaction products were separated by 10% (v/v) polyacrylamide gel electrophoresis under denaturing conditions. The gel was stained with toluidine blue and dried (left). The ^{14}C-labeled RNAs were detected with a phosphorimager (right). (**D**) *In vitro* methylations of $tRNA^{His}$ species isolated from HEK293T, KO1 and KO2 cells, and those of $tRNA^{His}$ species from rescued KO1 and KO2 cells with exogenous expression of BCDIN3D (KO1+BCDIN3D and KO2+BCDIN3D). $tRNA^{His}$ species after the reaction were separated by polyacrylamide gel electrophoresis, and the gel was stained with toluidine blue (upper). The ^{14}C-labeled $tRNA^{His}$ species were detected with a phosphorimager (lower), and the relative ^{14}C-band intensities were calculated. The intensity of $tRNA^{His}$ from KO1 was designated as 100. (**E**, **F**) LC/MS analysis of $tRNA^{His}$ isolated from KO1 and KO2. The RNase A-digested fragments of $tRNA^{His}$ were analyzed by LC/MS. The 5′-mp$G_{-1}G_1C_2$p is not detected in $tRNA^{His}$ from KO1 and KO2. The 5′-mp$G_{-1}G_1C_2$p was partially restored by the exogenous expression of BCDIN3D in the KO cells (KO1+BCDIN3D and KO2+BCDIN3D).

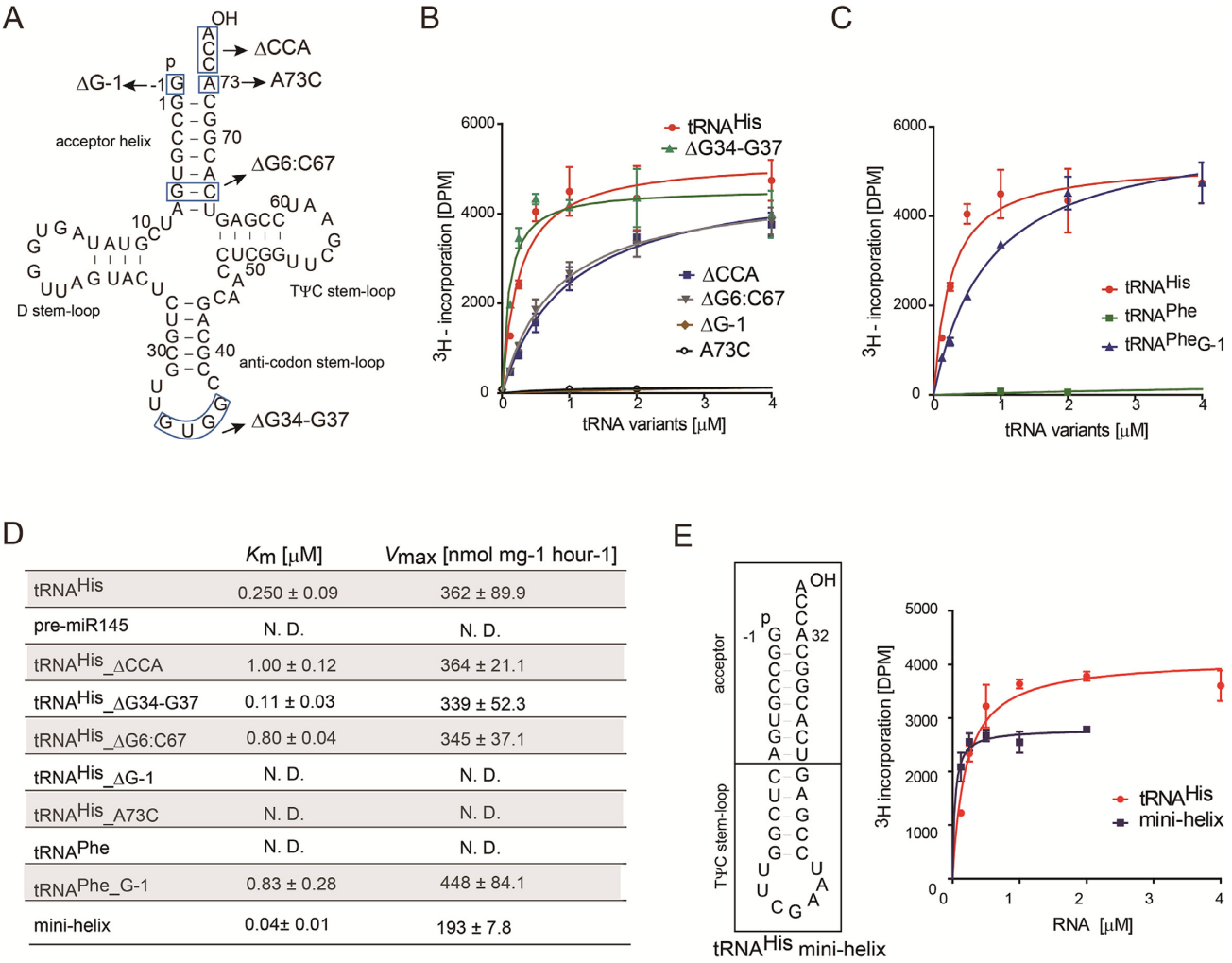

D

	K_m [μM]	V_{max} [nmol mg-1 hour-1]
tRNA^{His}	0.250 ± 0.09	362 ± 89.9
pre-miR145	N. D.	N. D.
tRNA^{His}_ΔCCA	1.00 ± 0.12	364 ± 21.1
tRNA^{His}_ΔG34-G37	0.11 ± 0.03	339 ± 52.3
tRNA^{His}_ΔG6:C67	0.80 ± 0.04	345 ± 37.1
tRNA^{His}_ΔG-1	N. D.	N. D.
tRNA^{His}_A73C	N. D.	N. D.
tRNA^{Phe}	N. D.	N. D.
tRNA^{Phe}_G-1	0.83 ± 0.28	448 ± 84.1
mini-helix	0.04± 0.01	193 ± 7.8

Figure 4. tRNA^{His} recognition by BCDIN3D. (**A**) Nucleotide sequences of the human cytoplasmic tRNA^{His} transcript and its variants used for biochemical analyses. (**B**) The steady-state kinetics of the methylation of the 5′-monophosphate of tRNA^{His} variants. Reaction mixtures containing various concentrations of tRNA^{His} and its variants [(tRNA^{His}_ΔG$_{-1}$, tRNA^{His}_ΔCCA, tRNA^{His}_ΔG$_6$:C$_{67}$, and tRNA^{His}_Δ32-35; 0.125–4 μM) and (tRNA^{His}_ΔG$_{-1}$, tRNA^{His}_A$_{73}$C; 1–15 μM)] were incubated at 37°C for 10 min. (**C**) The steady-state kinetics of human cytoplasmic tRNA^{Phe} and its variant. Reaction mixtures containing various concentrations of tRNA^{Phe} (1–15 μM) and its variant (tRNA^{Phe}_G$_{-1}$: 0.125–4 μM) were incubated at 37°C for 10 min. (**D**) Summary of kinetic parameters. N.D. (Not Determined). (**E**) Mini-helix of tRNA^{His} (left). The steady-state kinetics of the methylation of the 5′-monophosphate of the tRNA^{His} mini-helix with G$_{-1}$. Reaction mixtures containing various concentrations of tRNA^{His} and tRNA^{His} mini-helix (0.125–2 μM) were incubated at 37°C for 10 min (right). (**F**) Time courses of methyl-group transfer from AdoMet to tRNA^{His} mini-helix variants (G$_{-1}$, A$_{-1}$, C$_{-1}$ and U$_{-1}$) under standard conditions (1 μM RNA substrate and 0.1 μM recombinant BCDIN3D). (**G**) *In vitro* methylation of tRNA^{His} mini-helix variants at 37°C for 2 h. After the reaction, the RNA was purified by phenol–chloroform treatment and separated by 10% (v/v) polyacrylamide gel electrophoresis under denaturing conditions. The gel was stained with toluidine blue (left), dried and exposed to a BASS2000 imaging plate (Fujifilm, Japan) for 12 h (right). The bars in the graphs in (B), (C), (E) and (F) are SD of three independent experiments.

are 28, 1 and 1%, respectively, of that of the $tRNA^{His}$ mini-helix with G_{-1}, at the reaction end points (Figure 4F, G). Thus, the order of nucleotide preference at position −1 of the $tRNA^{His}$ mini-helix is $G_{-1} > A_{-1} >> C_{-1}, U_{-1}$. In addition to the G_{-1}–A_{73} mis-pair at the top of the acceptor helix of $tRNA^{His}$, the guanine base at position −1 would be recognized by BCDIN3D at the methylation step of the 5′-monophosphate of $tRNA^{His}$.

Except for $tRNA^{His}$, there are no other cytoplasmic tRNAs with an eight-nucleotide acceptor helix and a mis-pair at the top of the acceptor stem. Thus, BCDIN3D recognizes these unique structural features of the acceptor helix of cytoplasmic $tRNA^{His}$, and discriminates $tRNA^{His}$ from other tRNA species.

Effects of 5′-phosphate methylation of $tRNA^{His}$ on aminoacylation

The effects of the methyl group at the 5′-monophosphate of $tRNA^{His}$ on the aminoacylation by histidine-tRNA synthetase (HisRS) were examined *in vitro*, and the steady-state kinetic parameters were estimated (Figure 5A). The K_m value of 5′mp-$tRNA^{His}$ ($tRNA^{His}$ with 5′-monomethylmonophosphate) is about 1.5-fold of that of 5′p-$tRNA^{His}$ ($tRNA^{His}$ with 5′-monophosphate). The V_{max} value of 5′mp-$tRNA^{His}$ is about 1.5-fold of that of 5′p-$tRNA^{His}$. These results suggest that the introduction of the methyl-group on the 5′-monophosphate reduces the affinity of $tRNA^{His}$ toward HisRS, and increases the turnover of HisRS. The increased K_m of 5′mp-$tRNA^{His}$ is consistent with biochemical and recent structural analyses of the complex of eubacterial HisRS and $tRNA^{His}$ (28,29). In the structures, the 5′-monophosphate of $tRNA^{His}$ is strictly recognized by HisRS by hydrogen bonds. The reduced negative charge of the 5′-monophosphate by methylation would decrease the affinity of $tRNA^{His}$ toward HisRS, but enhance the structural changes of $tRNA^{His}$ (or enzyme) required for the catalysis. However, since the overall aminoacylation efficiencies (V_{max}/K_m value) are almost the same between 5′p-$tRNA^{His}$ and 5′mp-$tRNA^{His}$ (Figure 5A), the BCDIN3D activity is not indispensable for the aminoacylation process.

Effects of 5′-phosphate methylation of $tRNA^{His}$ on its stability *in vivo* and *in vitro*

To elucidate the function of the 5′-monomethylmonophosphate of cytoplasmic $tRNA^{His}$ in terms of its stability *in vivo*, the steady-state levels of $tRNA^{His}$ species in wild-type HEK293T and BCDIN3D knockout (KO1 and KO2) cells were analyzed by northern blotting. The results demonstrated that the methylation of the 5′-phosphate does not affect the steady state level of $tRNA^{His}$ *in vivo* (Figure 5B). Furthermore, to examine the stability of $tRNA^{His}$ *in vivo*, the KO cells were treated with actinomycin-D to inhibit global transcription. Under the assay conditions, the U6 snRNA degraded in a time-dependent manner over the twelve-hour period, in wild-type HEK293T and KO cells. The cytoplasmic $tRNA^{His}$ species from KO cells were stable over twelve hours after the actinomycin-D treatment, and no significant rapid decay of $tRNA^{His}$ in the KO cells was observed, as compared with $tRNA^{His}$ from wild-type HEK293T cells (Figure 5C).

However, an *in vitro* decay assay using cytoplasmic extracts revealed that $tRNA^{His}$ with the 5′-monophosphate (5′p-$tRNA^{His}$) is more rapidly degraded than $tRNA^{His}$ with the 5′-monomethylated phosphate (5′mp-$tRNA^{His}$) (Figure 5D). The half-lives of 5′p-$tRNA^{His}$ and 5′mp-$tRNA^{His}$ are estimated to be approximately 71 and 109 min, respectively. This result suggests that the 5′-monomethylmonophosphate of $tRNA^{His}$ protects it from degradation or dephosphorylation. Since BCDIN3D is localized in the cytoplasm (9), 5′ to 3′-exonucleases and/or phosphatases would be cooperatively involved in the degradation of 5′p-$tRNA^{His}$. The differences in the stabilities of $tRNA^{His}$ between the *in vivo* and *in vitro* analyses are discussed below.

DISCUSSION

In this study, we identified cytoplasmic $tRNA^{His}$ as a target of BCDIN3D. Our results showed that human cytoplasmic $tRNA^{His}$ tightly binds to BCDIN3D *in vivo* (Figure 1B), and has a 5′-monomethymonophosphate (Figure 1E, F), as previously reported (23). Human BCDIN3D efficiently monomethylates the 5′-monophosphate of cytoplasmic $tRNA^{His}$ *in vitro* (Figure 2A), and BCDIN3D is responsible for the modification in HEK293T cells (Figure 3C–E). BCDIN3D recognizes the unique features of cytoplasmic $tRNA^{His}$ *in vitro* (Figure 4B, C). In particular, BCDIN3D recognizes G_{-1} itself and the eight-nucleotide acceptor helix with the G_{-1}–A_{73} mis-pair at the top of the helix (Figure 4E, F). Except for cytoplasmic $tRNA^{His}$, there is no other cytoplasmic tRNA species with these unique structural features. Thus, BCDIN3D discriminates $tRNA^{His}$ from other tRNA species, and can act as a $tRNA^{His}$-specific 5′-monophosphate monomethyltransferase. It is not clear whether G_{-1} of $tRNA^{His}$ forms non-Watson–Crick hydrogen-bonds with A_{73}. A variety of non-Watson–Crick G:A pairings have been found in RNA structures and RNA–protein complex structures (30). The involvement of G_{-1}:A_{73} non-Watson–Crick hydrogen-bonds in the methylation of the 5′-monophosphate of $tRNA^{His}$ by BCDIN3D would be clarified by the structural analysis of BCDIN3D complexed with $tRNA^{His}$.

Recently, it was reported that human BCDIN3D dimethylates the 5′-monophosphate of a specific group of pre-miRNAs, such as pre-miR145 and pre-miR23b, *in vitro* (9). However, our *in vitro* results revealed that BDIN3D monomethylates the 5′-monophosphate of cytoplasmic $tRNA^{His}$ more efficiently than the 5′-monophosphate of pre-miR145 by over two orders of magnitude (Figure 2B, E), and neither cytoplasmic $tRNA^{His}$ nor pre-miR145 is dimethylated under our assay conditions (Figure 2C, D). In the previous report (9), the methylation efficiency of the 5′-monophosphate of pre-miR145 was calculated to be <1% of the input pre-miR145 substrate at the reaction end point. The low methylation efficiency of pre-miR145 is consistent with our results (Figure 2B, E).

In BCDIN3D knockout cells derived from HEK293T cells, the expression level of mature miR145 is not up-regulated, as compared with that in wild-type HEK293T

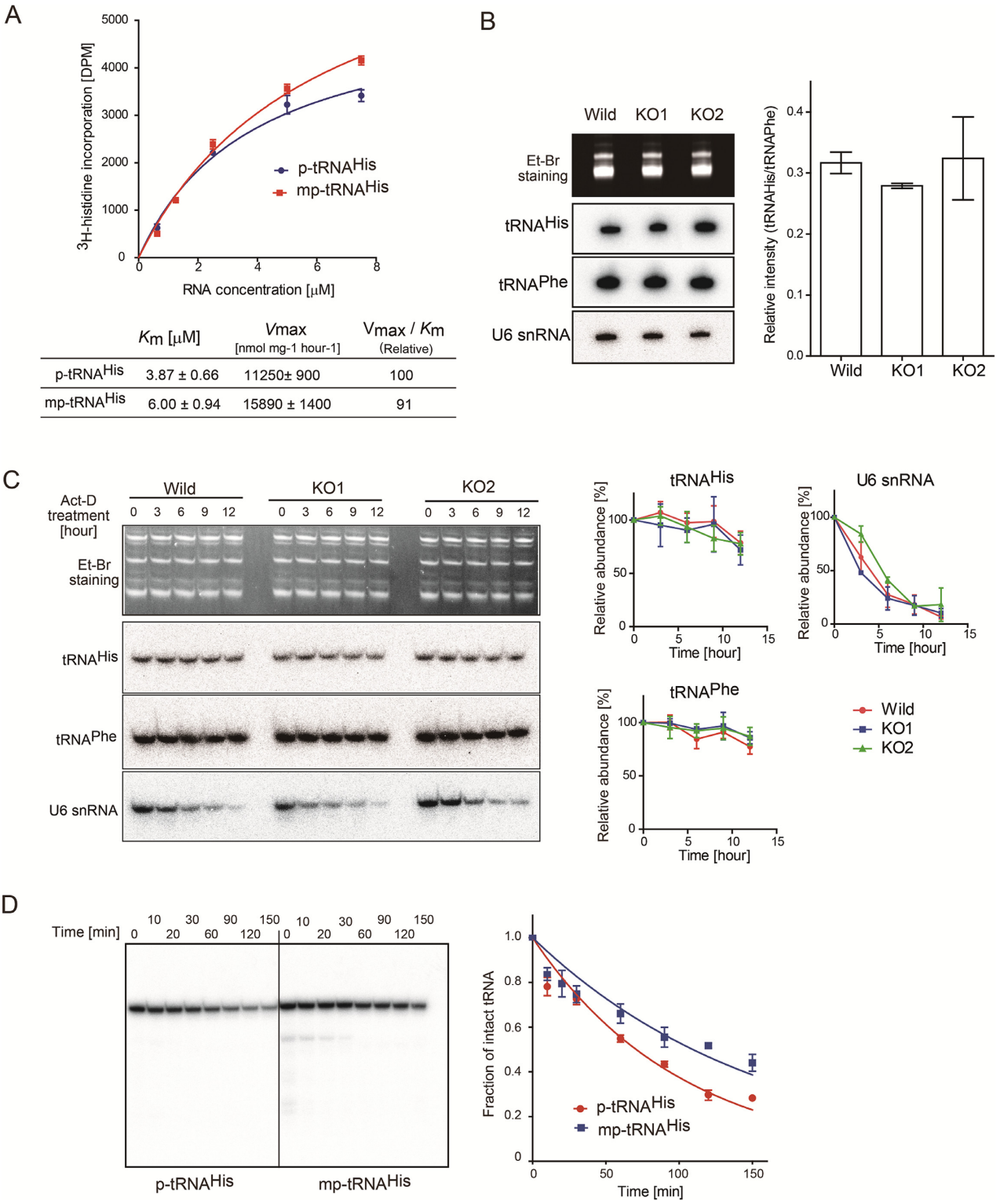

	K_m [μM]	Vmax [nmol mg-1 hour-1]	Vmax / Km (Relative)
p-tRNA^{His}	3.87 ± 0.66	11250± 900	100
mp-tRNA^{His}	6.00 ± 0.94	15890 ± 1400	91

Figure 5. Stability of tRNA^{His} with 5′-monomethylmonophosphate. (**A**) Aminoacylation of p-tRNA^{His} and mp-tRNA^{His} by histidine tRNA synthetase *in vitro*. The steady-state kinetics parameters were calculated. (**B**) Steady-state levels of tRNA^{His} species in wild-type (HEK293T) and BCDIN3D knockout cells (KO1 and KO2). The amounts of tRNA^{His} in wild-type HEK293, KO1 and KO2 cells were analyzed by northern blotting. Quantification of the ratios of the band intensities of tRNA^{His} and tRNA^{Phe}. (**C**) *In vivo* stabilities of tRNA^{His}. Wild-type HEK293T and KO cells were treated with actinomycin-D (Act-D) for 12 h. The stabilities of tRNA^{His} from the cells were analyzed by northern blotting, and quantified. The intensities of the bands of tRNA^{His} (or tRNA^{Phe} or U6 snRNA) at zero time were designated as 1.0, and the relative amount of tRNA^{His} (or tRNA^{Phe} or U6 snRNA) was quantified. (**D**) The *in vitro* decay of tRNA^{His} species with 5′-monomethylmonophosphate (5′pm-tRNA^{His}) and with 5′-monophosphate (5′p-tRNA^{His}) was performed using cytoplasmic extracts, and the amounts of intact tRNA^{His} species were quantified. The intensities of the bands of intact ^{32}P-tRNA^{His} at zero time were designated as 1.0, and the relative amounts of tRNA^{His} were quantified. Bars in graphs in (A)–(D) are SD of more than three independent experiments.

cells (Supplementary Figure S6A). In addition, the expression of BCDIN3D in HEK293T cells does not downregulate the expression of mature miR145 (Supplementary Figure S6B). These observations are distinct from those in a recent report showing that, in MCF-7 breast cancer cells, the knock-down of BCDIN3D by siRNA results in the upregulation of mature miR145 and the downregulation of pre-miR145 (9). The expression level of the BCDIN3D protein in HEK293T cells is higher than that in MCF-7 breast cancer cells (Supplementary Figure S7A). Since almost all of the cytoplasmic $tRNA^{His}$ is methylated even in MCF-7 cells, as in HEK293T and HeLa cells (Supplementary Figure S7B), the enzymatic activity and amount of BCDIN3D in MCF-7 cells are sufficient to methylate the 5′-phosphate of cytoplasmic $tRNA^{His}$. These observations suggest the absence of a direct co-relation between the expression levels of the BCDIN3D protein and miR145. Our *in vitro* results confirmed that BCDIN3D never dimethylates the 5′-monophosphate of either $tRNA^{His}$ or pre-miR145 (Figure 2). A recent report showed that synthetic pre-miR145 with a 5′-dimethylphosphate is poorly processed by Dicer *in vitro*, while synthetic pre-miR145 with a 5′-monomethylphosphate is processed by Dicer as efficiently as pre-miR145 with a 5′-phosphate (9). Thus, it is unlikely that miR145 expression is controlled by BCDIN3D, and the 5′-phosphate of pre-miR145 would not be dimethylated by BCDIN3D in HEK293T cells.

Collectively, the primary target of BCDIN3D is cytoplasmic $tRNA^{His}$, rather than pre-miRNAs, and BCDIN3D has monomethylation activity acting on the 5′-monophosphate of RNAs. Under specific conditions or in certain biological processes, the pre-miRNA might be methylated efficiently, and unknown regulatory factors specific to breast cancer cells might enhance the efficient pre-miRNA (di)methylation process *in vivo*. The *in vivo* mechanism of 5′-monophosphate dimethylation of specific pre-miRNAs, such as pre-miR145, in breast cancer cells awaits further studies.

The monomethylation of the 5′-monophosphate of cytoplasmic $tRNA^{His}$ increases both the K_m value of $tRNA^{His}$ toward HisRS and V_{max}, and the overall aminoacylation efficiencies by HisRS *in vitro* are not affected (Figure 5A). The steady-state levels of cytoplasmic $tRNA^{His}$ in HEK293T and BCDIN3D-knockout cells are not significantly different (Figure 5B, C). In human cells, under normal conditions, most tRNAs exist as aminoacyl-tRNAs and are protected by binding to elongation factor 1A (31,32). This may explain the similar stabilities of $tRNA^{His}$ in the wild-type and KO cells *in vivo* (Figure 5B, C). In contrast, the *in vitro* stability assay using cytoplasmic cell extracts showed that the 5′-monomethylation of the 5′-phosphate of the $tRNA^{His}$ transcript protects it from degradation (Figure 5D). Since the $tRNA^{His}$ transcript lacks the other post-transcriptional modifications (Figures 1D, 4A), it would be less stable than the native $tRNA^{His}$, and thus the effect of the 5′-monomethylation of the 5′-phosphate of $tRNA^{His}$ on its stability could be observed *in vitro*.

In the cytoplasm, 5′ to 3′ exonucleases, such as XRN1 requiring a 5′-monophosphate (33,34), might degrade $tRNA^{His}$ lacking a methylated 5′-monophosphate. However, there were no significant differences in the stabilities of $tRNA^{His}$ transcripts with or without a methyl-group at the 5′-phosphate, upon the treatment of $tRNA^{His}$ transcripts with recombinant yeast XRN1 (Supplementary Figure S8). Since the 5′-monomethylated phosphate of RNA is more resistant to the phosphatase, the dephosphorylation of the 5′-phosphate of $tRNA^{His}$ by some phosphatases and some other exonucleases in the extract would cooperatively degrade the $tRNA^{His}$ with a 5′-monophosphate. The G_{-1}–A_{73} mis-pair at the top of the $tRNA^{His}$ acceptor helix would allow these enzymes to access the 5′-end of $tRNA^{His}$. The identification of the enzymes responsible for the degradation of $tRNA^{His}$ awaits further studies.

The involvement of the 5′-monomethylation of cytoplasmic $tRNA^{His}$ by BCDIN3D in the tumorigenic phenotype of breast cancer cells still remains elusive. Recent studies have shown that the expression levels of specific tRNAs, such as initiator $tRNA^{Met}$, are elevated in breast cancer cells (35). The upregulation of specific tRNAs, such as $tRNA^{Glu}UUC$ and $tRNA^{Arg}CCG$, reportedly stabilizes mRNAs containing the corresponding codons and enhances the translation in highly metastatic breast cancer cells (36). However, the steady state level of cytoplasmic $tRNA^{His}$ is not affected by the knockdown of BCDIN3D in HEK293T cells (Figure 5B, C). Recent studies have also provided evidence that tRNA fragments (tRFs), produced under stress conditions, participate in various cellular functions beyond their established roles in protein synthesis (37,38). In breast and prostate cancers, specific tRNAs are cleaved by angiogenin, an RNaseA-type nuclease, and tRNA halves are abundantly expressed in a sex hormone-dependent manner (39). Interestingly, about 27% of the tRNA halves are the 5′-half of $tRNA^{His}$, while about 60% are the 5′-half of $tRNA^{Lys}$. These tRNA halves have been shown to promote the proliferation of breast and prostate cancer cells, by unknown mechanisms. In human and mouse cells, 3′- or 5′-terminal tRFs (3′-tRF or 5′-tRF) reportedly accumulate in an asymmetric manner (40), and these tRFs associate with Ago2 and downregulate their target genes by cleaving their transcripts (41). The 3′-tRF, but not the 5′-tRF, derived from cytoplasmic $tRNA^{His}$ is complementary to human endogeneous retroviral sequences in the genome (41). It would be interesting to determine whether the 5′-monomethylation of the 5′-monophosphate of $tRNA^{His}$ controls the expression of tRNA halves and tRFs derived from $tRNA^{His}$ in breast cancer cells or under specific biological or stress conditions. Future work will clarify whether the methylation of the 5′-phosphate of $tRNA^{His}$ by BCDIN3D is involved in the tumorigenic phenotypes of breast cancer and other cancers.

SUPPLEMENTARY DATA

Supplementary Data are available at NAR Online.

ACKNOWLEDGEMENTS

We thank Yuka Fujimoto and Azusa Hamada for technical assistance.

FUNDING

Funding Program for Next Generation World-Leading Researchers of JSPS [to K.T.]; Grants-in-Aid for Scientific Research (A) [to K.T.] from JSPS and a Grant-in-Aid for Scientific Research on Innovative Areas from Ministry of Education, Science, Sports and Culture of Japan [to K.T., T.S.]; Takeda Science Foundation, Astellas Foundation for Research on Metabolic Disorders and Hamaguchi Foundation for the Advancement of Biochemistry [to K.T.]. Funding for open access charge: Grant-in-Aid for Scientific Research on Innovative Areas from Ministry of Education, Science, Sports, and Culture of Japan [to K.T.].
Conflict of interest statement. None declared.

REFERENCES

1. Driever,W. and Nusslein-Volhard,C. (1989) The bicoid protein is a positive regulator of hunchback transcription in the early Drosophila embryo. *Nature*, **337**, 138–143.
2. Zhu,W. and Hanes,S.D. (2000) Identification of drosophila bicoid-interacting proteins using a custom two-hybrid selection. *Gene*, **245**, 329–339.
3. Cosgrove,M.S., Ding,Y., Rennie,W.A., Lane,M.J. and Hanes,S.D. (2012) The Bin3 RNA methyltransferase targets 7SK RNA to control transcription and translation. *Wiley Interdiscipl. Rev. RNA*, **3**, 633–647.
4. Singh,N., Morlock,H. and Hanes,S.D. (2011) The Bin3 RNA methyltransferase is required for repression of caudal translation in the Drosophila embryo. *Dev. Biol.*, **352**, 104–115.
5. Diribarne,G. and Bensaude,O. (2009) 7SK RNA, a non-coding RNA regulating P-TEFb, a general transcription factor. *RNA Biol.*, **6**, 122–128.
6. Peterlin,B.M., Brogie,J.E. and Price,D.H. (2012) 7SK snRNA: a noncoding RNA that plays a major role in regulating eukaryotic transcription. *Wiley Interdiscipl. Rev. RNA*, **3**, 92–103.
7. Jeronimo,C., Forget,D., Bouchard,A., Li,Q., Chua,G., Poitras,C., Thérien,C., Bergeron,D., Bourassa,S., Greenblatt,J. *et al.* (2007) Systematic analysis of the protein interaction network for the human transcription machinery reveals the identity of the 7SK capping enzyme. *Mol. Cell*, **27**, 262–274.
8. Shuman,S. (2007) Transcriptional networking cap-tures the 7SK RNA 5′-γ-methyltransferase. *Mol. Cell*, **27**, 517–519.
9. Xhemalce,B., Robson,S.C. and Kouzarides,T. (2012) Human RNA methyltransferase BCDIN3D regulates microRNA processing. *Cell*, **151**, 278–288.
10. Liu,R., Wang,X., Chen,G.Y., Dalerba,P., Gurney,A., Hoey,T., Sherlock,G., Lewicki,J., Shedden,K. and Clarke,M.F. (2007) The prognostic role of a gene signature from tumorigenic breast-cancer cells. *N. Engl. J. Med.*, **356**, 217–226.
11. Yao,L., Chi,Y., Hu,X., Li,S., Qiao,F., Wu,J. and Shao,Z.M. (2016) Elevated expression of RNA methyltransferase BCDIN3D predicts poor prognosis in breast cancer. *Oncotarget*, **7**, 53895–53902.
12. Sachdeva,M., Zhu,S., Wu,F., Wu,H., Walia,V. and Kumar,S. (2009) p53 represses c-Myc through induction of the tumor suppressor miR-145. *Proc. Natl. Acad. Sci. U.S.A.*, **106**, 3207–3212.
13. Shi,B., Sepp-Lorenzino,L., Prisco,M., Linsley,P., deAngelis,T. and Baserga,R. (2007) Micro RNA 145 targets the insulin receptor substrate-1 and inhibits the growth of colon cancer cells. *J. Biol. Chem.*, **282**, 32582–32590.
14. Spizzo,R., Nicoloso,M.S., Lupini,L., Lu,Y., Fogarty,J., Rossi,S., Zagatti,B., Fabbri,M., Veronese,A., Liu,X. *et al.* (2009) miR-145 participates with TP53 in a death-promoting regulatory loop and targets estrogen receptor-[alpha] in human breast cancer cells. *Cell Death Differ.*, **17**, 246–254.
15. Park,J.E., Heo,I., Tian,Y., Simanshu,D.K., Chang,H., Jee,D., Patel,D.J. and Kim,V.N. (2011) Dicer recognizes the 5′ end of RNA for efficient and accurate processing. *Nature*, **475**, 201–205.
16. Suzuki,T., Ikeuchi,Y., Noma,A., Suzuki,T. and Sakaguchi,Y. (2007) Mass spectrometric identification and characterization of RNA-modifying enzymes. *Methods Enzymol.*, **425**, 211–229.
17. Soma,A., Ikeuchi,Y., Kanemasa,S., Kobayashi,K., Ogasawara,N., Ote,T., Kato,J., Watanabe,K., Sekine,Y. and Suzuki,T. (2003) An RNA-modifying enzyme that governs both the codon and amino acid specificities of isoleucine tRNA. *Mol. Cell*, **12**, 689–698.
18. Pyzocha,N.K., Ran,F.A., Hsu,P.D. and Zhang,F. (2014) RNA-guided genome editing of mammalian cells. *Methods Mol. Biol.*, **1114**, 269–277.
19. Cong,L., Ran,F.A., Cox,D., Lin,S., Barretto,R., Habib,N., Hsu,P.D., Wu,X., Jiang,W., Marraffini,L.A. *et al.* (2013) Multiplex genome engineering using CRISPR/Cas systems. *Science (New York, N.Y.)*, **339**, 819–823.
20. Tsurui,H., Kumazawa,Y., Sanokawa,R., Watanabe,Y., Kuroda,T., Wada,A., Watanabe,K. and Shirai,T. (1994) Batchwise purification of specific tRNAs by a solid-phase DNA probe. *Anal. Biochem.*, **221**, 166–172.
21. Tomita,K., Ueda,T., Ishiwa,S., Crain,P.F., McCloskey,J.A. and Watanabe,K. (1999) Codon reading patterns in Drosophila melanogaster mitochondria based on their tRNA sequences: a unique wobble rule in animal mitochondria. *Nucleic Acids Res.*, **27**, 4291–4297.
22. Tomita,K., Ueda,T. and Watanabe,K. (1999) The presence of pseudouridine in the anticodon alters the genetic code: A possible mechanism for assignment of the AAA lysine codon as asparagine in echinoderm mitochondria. *Nucleic Acids Res.*, **27**, 1683–1689.
23. Rosa,M.D., Hendrick,J.P. Jr., Lerner,M.R., Steitz,J.A. and Reichlin,M. (1983) A mammalian tRNAHis-containing antigen is recognized by the polymyositis-specific antibody anti-Jo-1. *Nucleic Acids Res.*, **11**, 853–870.
24. Cooley,L., Appel,B. and Soll,D. (1982) Post-transcriptional nucleotide addition is responsible for the formation of the 5′ terminus of histidine tRNA. *Proc. Natl. Acad. Sci. U.S.A.*, **79**, 6475–6479.
25. Ohira,T. and Suzuki,T. (2016) Precursors of tRNAs are stabilized by methylguanosine cap structures. *Nat. Chem. Biol.*, **12**, 648–655.
26. Sander,J.D. and Joung,J.K. (2014) CRISPR-Cas systems for editing, regulating and targeting genomes. *Nat. Biotech.*, **32**, 347–355.
27. Gu,W., Jackman,J.E., Lohan,A.J., Gray,M.W. and Phizicky,E.M. (2003) tRNAHis maturation: an essential yeast protein catalyzes addition of a guanine nucleotide to the 5′ end of tRNAHis. *Genes Dev.*, **17**, 2889–2901.
28. Fromant,M., Plateau,P. and Blanquet,S. (2000) Function of the extra 5′-phosphate carried by histidine tRNA. *Biochemistry*, **39**, 4062–4067.
29. Tian,Q., Wang,C., Liu,Y. and Xie,W. (2015) Structural basis for recognition of G-1-containing tRNA by histidyl-tRNA synthetase. *Nucleic Acids Res.*, **43**, 2980–2990.
30. Hermann,T. and Westhof,E. (1999) Non-Watson-Crick base pairs in RNA-protein recognition. *Chem. Biol.*, **6**, R335–R343.
31. Petrushenko,Z.M., Budkevich,T.V., Shalak,V.F., Negrutskii,B.S. and El'skaya,A.V. (2002) Novel complexes of mammalian translation elongation factor eEF1A.GDP with uncharged tRNA and aminoacyl-tRNA synthetase. Implications for tRNA channeling. *Eur. J. Biochem. / FEBS*, **269**, 4811–4818.
32. Negrutskii,B.S. and El'skaya,A.V. (1998) Eukaryotic translation elongation factor 1 alpha: structure, expression, functions, and possible role in aminoacyl-tRNA channeling. *Progr. Nucleic Acid Res. Mol. Biol.*, **60**, 47–78.
33. Chernyakov,I., Whipple,J.M., Kotelawala,L., Grayhack,E.J. and Phizicky,E.M. (2008) Degradation of several hypomodified mature tRNA species in Saccharomyces cerevisiae is mediated by Met22 and the 5′-3′ exonucleases Rat1 and Xrn1. *Genes Dev.*, **22**, 1369–1380.
34. Wu,J. and Hopper,A.K. (2014) Healing for destruction: tRNA intron degradation in yeast is a two-step cytoplasmic process catalyzed by tRNA ligase Rlg1 and 5′-to-3′ exonuclease Xrn1. *Genes Dev.*, **28**, 1556–1561.
35. Pavon-Eternod,M., Gomes,S., Rosner,M.R. and Pan,T. (2013) Overexpression of initiator methionine tRNA leads to global reprogramming of tRNA expression and increased proliferation in human epithelial cells. *RNA (New York, N.Y.)*, **19**, 461–466.
36. Goodarzi,H., Nguyen,H.C., Zhang,S., Dill,B.D., Molina,H. and Tavazoie,S.F. (2016) Modulated expression of specific tRNAs Drives gene expression and cancer progression. *Cell*, **165**, 1416–1427.
37. Gebetsberger,J. and Polacek,N. (2013) Slicing tRNAs to boost functional ncRNA diversity. *RNA Biol.*, **10**, 1798–1806.

38. Sobala,A. and Hutvagner,G. (2011) Transfer RNA-derived fragments: origins, processing, and functions. *Wiley Interdiscipl. Rev. RNA*, **2**, 853–862.
39. Honda,S., Loher,P., Shigematsu,M., Palazzo,J.P., Suzuki,R., Imoto,I., Rigoutsos,I. and Kirino,Y. (2015) Sex hormone-dependent tRNA halves enhance cell proliferation in breast and prostate cancers. *Proc. Natl. Acad. Sci. U.S.A.*, **112**, E3816–E3825.
40. Kumar,P., Mudunuri,S.B., Anaya,J. and Dutta,A. (2015) tRFdb: a database for transfer RNA fragments. *Nucleic Acids Res.*, **43**, D141–D145.
41. Li,Z., Ender,C., Meister,G., Moore,P.S., Chang,Y. and John,B. (2012) Extensive terminal and asymmetric processing of small RNAs from rRNAs, snoRNAs, snRNAs, and tRNAs. *Nucleic Acids Res.*, **40**, 6787–6799.